Chemical Physics Letters 610–611 (2014) 381–387

Contents lists available at ScienceDirect

Chemical Physics Letters

journal homepage: www.elsevier.com/locate/cplett

Adsorption of methanethiol on Au(1 1 1): Role of hydrogen bonds

P.G. Lustemberg[a,*], P.N. Abufager[a], M.L. Martiarena[b], H.F. Busnengo[a]

[a] Instituto de Física Rosario (CONICET-UNR) and Facultad de Ciencias Exactas, Ingeniería y Agrimensura, Universidad Nacional de Rosario, Av. Pellegrini 250, 2000 Rosario, Argentina
[b] Centro Atómico Bariloche (CNEA), Instituto Balseiro (UNCuyo) and CONICET, Av. Bustillo 9500, 8400 San Carlos de Bariloche, Río Negro, Argentina

ARTICLE INFO

Article history:
Received 21 May 2014
In final form 28 July 2014
Available online 4 August 2014

ABSTRACT

Through Density Functional Theory calculations (with and without long range dispersion corrections) we investigate and compare the stability of a large set of structures involving methanetiol molecularly adsorbed on Au(1 1 1). In particular, we consider possible cooperative effects like the formation of dimers and chains of molecules interacting through SH···SH H-bonds. We conclude that structures of dimer H-bonds are the most stable ones for molecular coverages $1/6 \lesssim \theta \leq 1/3$. For this range of coverages, a dimer H-bond moiety can act as a precursor for the S-H bond scission process through a cooperative H transfer mechanism.

1. Introduction

The great range of possible technological applications of self-assembled monolayers (SAMs) formed by alkanethiols, $HS(CH_2)_{n-1}CH_3$, deposited on surfaces have motivated a huge number of experimental and theoretical studies during the last years (see e.g. [1–6] and references therein). Many studies have been focused on the structure and stability of monolayers involving chemisorbed thiolates formed after the scission of the S-H bond see e.g. [6,7]. However, some attention has been also payed to molecularly adsorbed states because they are often considered possible precursors for the S-H bond scission process.

For $HSCH_3$, low temperature scanning tunneling microscopy (STM) experiments indicate that the molecules adsorb almost flat on the surface with the S atom on top of a single Au atom (i.e. on a top site) [8–10]. At low coverages and 5K, Maksymovych etal. [8] observed dimers of $HSCH_3$ molecules after using the STM tip to apply a voltage pulse on individually adsorbed molecules in order to approach them to each other. From the analysis of the STM images and Density Functional Theory (DFT) calculations, it was proposed that the observed dimers are formed by two molecules sit on nearest neighbor Au atoms. Nenchev etal. [10] observed spontaneous dimerization of intact $HSCH_3$ molecules on Au(1 1 1) for a wide range of coverages. Based on DFT calculations, the authors suggested that these dimers might consist in one molecule adsorbed with the S atom near a top site and the other over a bridge site. However, the very small energy gain associated with the formation of such dimers and the lack of dispersion effects in their DFT calculations did not allow the authors to unambiguously conclude about the precise structure of the dimers observed in the STM images [10].

Though hydrogen bond (H-bond) interaction between alkanethiols are expected to be weaker than between molecules containing oxygen atoms (e.g. alcohols), there exists in the literature evidence of its effect on the SH infrared absorption mode frequency [11] and association of several thiols in carbon tetrachloride and chlorobenzene [12]. More recently, Russell etal. [13] observed the formation of dimers of H_2S molecules bound through H-bonds on Ag(1 1 1), and Askerka etal. [14] concluded that H-bonds can stabilize dimers of methanethiol molecules adsorbed on Au_{20} clusters, favoring the S-H bond scission.

The latter results suggest that the often neglected role of H-bonds on the molecular adsorption and dissociation of alkanethiols on Au(1 1 1) might be more important than expected. To the best of our knowledge, no systematic study on the role of intermolecular H-bonds between methanethiol molecules adsorbed on Au(1 1 1) and its possible connection with the dimers observed in STM experiments has been reported. In this paper we report a study based on DFT calculations (with and without dispersion corrections) of a large set of structures of methanethiol molecules on Au(1 1 1) from small coverages up to a full monolayer. We show that for coverages close to saturation, dimers of methanethiol molecules bound through a SH···SH bond give rise to the most stable adsorption structures. Moreover, we show that this Dimer-H-bond plays the role of precursor state for the S-H bond scission through a concerted H-transfer reaction pathway. The paper is organized as follows. In

* Corresponding author.
E-mail addresses: lustemberg@ifir-conicet.gov.ar, lustemberg@gmail.com (P.G. Lustemberg).

http://dx.doi.org/10.1016/j.cplett.2014.07.064
0009-2614/

Section 2 we describe the methods employed in the present calculations. Then, in Section 3 we present the results and discussions, and finally in Section 4 we summarize the conclusions of our study.

2. Computational details

All the DFT calculations were carried using the slab-supercell approach [15], within the generalized gradient approximation (GGA) proposed by Perdew, Burke and Ernzerhof (PBE) [16] to account electronic exchange and correlation (XC). The one-electron Khon-Sham orbitals have been expanded in a plane wave basis set (with a cut-off energy of 400 eV) and the electron-core interaction has been represented within the projected augmented wave (PAW) method [17]. Electron smearing was introduced following the Methfessel-Paxton technique [18] with σ = 0.2 eV, and the total energies were extrapolated to 0 K.

The Monkhorst-Pack method [19] was employed to select k-point meshes in reciprocal space characterized by a density (for all the unit cells considered) equal to or slightly higher than the one corresponding to a $25 \times 25 \times 1$ k-points mesh for a 1×1 cell of the Au(1 1 1) surface: e.g. $5 \times 5 \times 1$ for a 5×5 cell, $9 \times 9 \times 1$ for a 3×3 cell, $13 \times 9 \times 1$ for a 2×3 cell, etc. All the calculations were spin-restricted, and have been carried out with the Vienna Ab-initio Simulation Program (VASP) [20–24].

In order to introduce long-range dispersion corrections we have used the so called DFT-D2 approach proposed by Grimme [25]. Thus, the total energy is written as a sum of the DFT-PBE total energy, E^{PBE}, plus a sum of long-range pairwise potentials between atoms as follows:

$$E = E^{PBE} + s_6 \sum_{i \neq j} f_{SO}(r_{ij}) \frac{C_{ij}}{r_{ij}^6}. \quad (1)$$

In Eq. (1) s_6 is a global scaling factor (equal to 0.75 for PBE), r_{ij} is the distance between atoms i and j, and f_{SO} is the switch-off function:

$$f_{SO}(r_{ij}) = \frac{1}{1 + e^{-d(r_{ij}/R_{ij} - 1)}} \quad (2)$$

introduced to avoid short-range corrections to the DFT total energies. The C_{ij} and R_{ij} parameters for a pair of atoms i and j were taken, as usual, using the expressions:

$$C_{ij} = \sqrt{C_i C_j} \quad (3)$$

and

$$R_{ij} = \frac{R_i + R_j}{2}, \quad (4)$$

being C_i and R_i species-specific parameters whose values for H, S and C have been taken from ref. [25]. For Au, we have used the values proposed and validated by Gross et al. [26] from the use of a QM:QM hybrid approach: i.e. C_{Au}=21.227 J nm^6/mol (220 eV Å^6), and R_{Au}=1.772 Å.

All geometry optimizations were carried out using both the conjugate-gradient and quasi-Newton minimization methods. The resulting equilibrium bond lengths for $HSCH_3$ in vacuum are: d_{S-C} = 1.82 Å, d_{S-H} = 1.35 Å, d_{C-H} = 1.10 Å, whereas the angle between the adjacent bonds θ_{C-S-H} is 96.8 °. All these theoretical structural parameters are in excellent agreement with the experimental values reported in ref. [27]: d^{exp}_{S-C} = 1.82 Å, d^{exp}_{S-H} = 1.34 Å, d^{exp}_{C-H} = 1.09 Å, and θ^{exp}_{C-S-H} = 96.5 °. The theoretical lattice constant obtained for Au bulk (using a $25 \times 25 \times 25$ k-point mesh) was a_{Au} = 4.115 Å, also in good agreement with the experimental value, a^{exp}_{Au} = 4.08 Å[28]. The Au(1 1 1) surface was represented by a four-layer (one mobile and three fixed) slab separated from its periodic images by a vacuum region of ~ 21 Å. The optimization of the distance between the two outermost layers of the slab gave an almost negligible contraction with respect to the value in Au bulk as usual for the closest packed 1 1 1 faces of face centered cubic metals. During the geometry optimizations we have allowed the relaxation of all the atoms of the molecules and the Au atoms in the surface topmost layer (i.e. we have kept fixed the positions of all the other Au atoms as in bulk).

The adsorption energy per molecule, ε, has been computed using the expression:

$$\varepsilon = \frac{1}{N}[E_{NMet@Au(1\,1\,1)} - E_{Au(1\,1\,1)} - NE_{Met}], \quad (5)$$

where N is the number of methanethiol molecules per unit cell, and $E_{NMet@Au(1\,1\,1)}$, $E_{Au(1\,1\,1)}$ and E_{Met} are the total energies of the N-molecule/Au(1 1 1) system, the clean Au(1 1 1) surface, and a single methanethiol molecule in vacuum, respectively. Thus, negative ε values correspond to exothermic adsorption. Test calculations indicate that the selected DFT settings (k-points, energy cut-off, etc.) give rise to errors of the ε values, smaller than 0.01 eV.

In order to search dissociation minimum energy pathways and the corresponding transition states (TS), we have employed the climbing image nudged elastic band method (CI-NEB) [29–33] followed by a minimization of the forces on each atom using the quasi-Newton algorithm implemented in VASP. For every resulting TS configuration, we have diagonalized the Hessian matrix of the molecule-surface potential energy surface and verified the existence of only one imaginary frequency.

3. Results and discussions

It is well established that a single methanethiol molecule adsorbs on Au(1 1 1) with the S atom approximately on top of a Au atom (d_{S-Au} ~ 2.6 Å), the S-H and S-C bonds almost parallel to the surface and the methyl group on a hollow site (but it can rotate almost freely around the S atom) [34,3,5]. In order to investigate possible cooperative interactions between methanethiol molecules on Au(1 1 1) we have considered a large set of structures involving molecules:

1. adsorbed on top sites and with the distance between the S atoms of nearest neighbor (NN) molecules larger than ~5 Å; i.e. avoiding adsorption on top of NN Au atoms, (hereafter referred to as *Monomer structures*)
2. adsorbed with the S atom of NN molecules on top of NN Au atoms (hereafter referred to as *Dimer structures*),
3. forming dimers through an H-bond S-H···S-H and with the two S atoms of this dimer separated from the S atom of any other molecule by more than ~5 Å, (hereafter referred to as *Dimer-H-bond structures*), and
4. forming a chain of molecules connected with each other through an H-bond S-H···S-H, (hereafter referred to as *Chain-H-bond structures*).

In Figure 1 we show a representative example of each kind of structures considered. Panels a and b correspond to a Monomer- and Dimer-structure, respectively. The positions of the two molecules forming a Dimer-H-bond is shown in panel c. This structure is very similar to the optimum one obtained for two methanethiol molecules in vacuum. One molecule (that plays the role of H donor) is closer to the surface and adopts a geometry similar to the monomer shown in Figure 1a (i.e. approximately flat on the surface and with the S atom near a top site). The other molecule (that plays the role of H-acceptor) is further away from the surface and the S-H bond points to the surface (Fig. 1c). Finally, in the Chain-H-bond structures (Fig. 1d) one every two molecules is in a configuration similar to the monomer (Fig. 1a) whereas the other (further away from the surface) has its S atom near a hollow site.

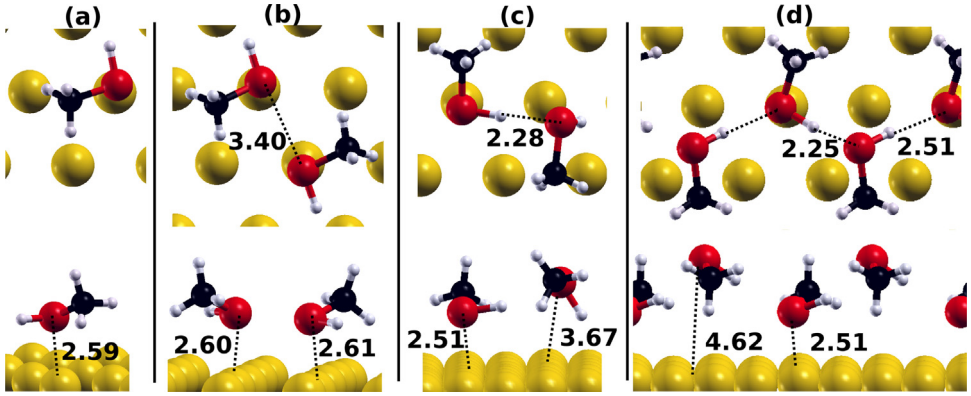

Fig. 1. Top and side view of the different kind of molecular states investigated: (a) Monomer, (b) Dimer, (c) Dimer-H-bond, and (d) Chain-H-bond states. Red atoms: S, black atoms: C, white atoms: H, and yellow atoms: Au. Some relevant inter-atomic distances for each structure are given in Angstroms. (For interpretation of the references to color in this figure legend, the reader is referred to the web version of this article.)

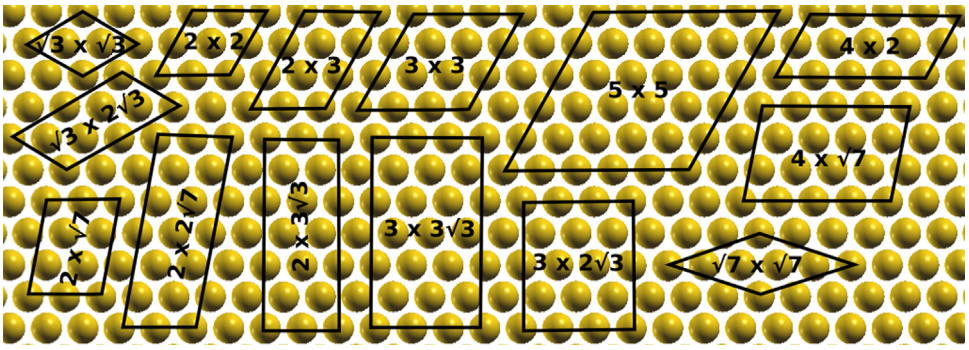

Fig. 2. Schematic illustration of the Au(1 1 1) surface showing the different unit cells used to carry out the DFT calculations.

Since we are interested in coverages $0 \lesssim \theta \lesssim 1/3$, the four kind of structures listed above (i-iv) were investigated in the unit cells represented in Figure 2 and with different number of molecules per cell. The binding energies per molecule as well as the shortest S-S and S-Au distances (d_{S-S} and d_{S-Au} respectively), for each structure are listed in Tables 1, 2, 3, and 4. When there is more than a single molecule per cell, in the tables we included all the values of d_{S-S} and d_{S-Au} found in each structure.

For Monomers (Table 1), ε barely changes with coverage for $1/25 \leq \theta \leq 1/8$ but increases significantly when θ further increases.

Table 1
Average adsorption energies, ε, for Monomer structures (see text). For each structure we provide unit cell employed, the number of molecules per cell, N, the nearest neighbor S-S and S-Au distances, d_{S-S}, and d_{S-Au} respectively.

θ	Unit cell	N	d_{S-S} (Å)	d_{S-Au} (Å)	ε (eV)
1/25	5×5	1	14.55	2.59	−0.75
1/18	$3 \times 3\sqrt{3}$	1	8.73	2.59	−0.74
	$4 \times \sqrt{7}$	1	7.70	2.59	−0.73
1/12	$3 \times 2\sqrt{3}$	1	8.73	2.60	−0.72
	$2 \times 3\sqrt{3}$	1	5.82	2.60	−0.73
	$2 \times 2\sqrt{7}$	1	5.82	2.59	−0.74
1/9	3×3	1	8.73	2.62	−0.70
1/8	2×4	1	5.82	2.60	−0.73
1/7	$\sqrt{7} \times \sqrt{7}$	1	7.70	2.63	−0.68
	$2\sqrt{3} \times \sqrt{3}$	1	5.04	2.65	−0.68
	$4 \times \sqrt{7}$	2	5.82	2.60; 2.60	−0.68
1/6	$2 \times \sqrt{7}$	1	5.82	2.62	−0.70
	2×3	1	5.82	2.63	−0.69
	$2 \times 2\sqrt{7}$	2	5.82	2.60; 2.63	−0.68
2/9	3×3	2	5.02	2.69; 2.68	−0.63
1/4	2×2	1	5.82	2.69	−0.66
1/3	$\sqrt{3} \times \sqrt{3}$	1	5.04	2.85	−0.60

In particular, for θ=1/3, ε is greater (less stable) than for the lowest coverages considered by ∼0.15 eV. This weakening of the $HSCH_3$-Au(1 1 1) bond is consistent with increasing values of d_{S-Au} when θ increases: $d_{S-Au} \sim$ 2.6 Åfor $\theta \lesssim$ 1/6, but d_{S-Au}=2.85 Åfor θ=1/3.

In the case of Dimers (Table 2), in all the structures considered the S-H bonds of both molecules point to opposite directions and the S atoms are slightly shifted away from top sites (approximately in opposite directions). This is the reason for the d_{S-S} values $\sim 0.5 - 0.6$ Ålarger than the Au-Au NN distance (Δ = 2.91 Å). This points to a weak repulsion between S atoms separated by a distance Δ. Still, in the whole range of coverages considered, these dimers are equally stable as monomers for the same coverage. In line with this, for any given coverage, the d_{S-Au} values for monomers and dimers are also close to each other (compare Tables 1 and 2). It must be mentioned that for the dimer in the $3 \times 2\sqrt{3}$ cell (θ = 1/6) our

Table 2
Idem Table 1 but for Dimer structures (see text).

θ	Unit cell	N	d_{S-S} (Å)	d_{S-Au} (Å)	ε (eV)
2/25	5×5	2	3.40	2.60; 2.61	−0.74
1/9	$3 \times 3\sqrt{3}$	2	3.42	2.63; 2.63	−0.72
	$4 \times \sqrt{7}$	2	3.38	2.63; 2.64	−0.70
1/6	$3 \times 2\sqrt{3}$	2	3.43	2.65; 2.66	−0.70
	$2 \times 3\sqrt{3}$	2	3.42	2.67; 2.70	−0.66
	$2 \times 2\sqrt{7}$	2	3.41	2.68; 2.68	−0.66
2/9	3×3	2	3.39	2.70; 2.71	−0.66
1/4	2×4	2	3.46	2.71; 2.74	−0.63
2/7	$\sqrt{7} \times \sqrt{7}$	2	3.44	2.73; 2.74	−0.63
1/3	2×3	2	3.27	2.80; 2.84	−0.58
	$2 \times \sqrt{7}$	2	3.47	2.76; 2.79	−0.60

Table 3
Idem Table 1 but for Dimer-H-bond structures (see text). Here we also report the S-H distance between the atoms involved in the H bond, $d_{SH\cdots SH}$.

θ	Unit cell	N	d_{S-S} (Å)	d_{S-Au} (Å)	$d_{SH\cdots SH}$ (Å)	ε (eV)
2/25	5×5	2	3.64	2.51; 3.67	2.28	−0.70
1/9	$3\times3\sqrt{3}$	2	3.67	2.52; 3.68	2.29	−0.70
1/6	$4\times\sqrt{7}$	2	3.64	2.52; 3.77	2.29	−0.70
	$3\times2\sqrt{3}$	2	3.67	2.52; 3.69	2.30	−0.68
	$2\times3\sqrt{3}$	2	3.64	2.52; 3.71	2.28	−0.70
	$2\times2\sqrt{7}$	2	3.64	2.52; 3.72	2.29	−0.71
2/9	3×3	2	3.68	2.54; 3.72	2.32	−0.68
1/4	2×4	2	3.67	2.52; 3.75	2.30	−0.70
2/7	$\sqrt{7}\times\sqrt{7}$	2	3.65	2.55; 3.79	2.31	−0.67
1/3	$2\sqrt{3}\times\sqrt{3}$	2	3.64; 3.68	2.54; 3.79	2.28	−0.69
	$2\times\sqrt{7}$	2	3.66	2.55; 3.80	2.32	−0.70
	2×3	2	3.72	2.56; 3.76	2.37	−0.70
	$2\times3\sqrt{3}$	4	3.64; 3.70 4.22	2.55; 2.56 3.69; 3.88	2.27; 2.40	−0.70
	$2\times2\sqrt{7}$	4	3.65; 3.65 4.71	2.55; 2.55 3.81; 3.81	2.31; 2.31	−0.71

values of d_{S-S} and d_{S-Au} are also in good agreement with the ones reported by Hagelberg et al. for the same structure [35]: 3.43 Åvs. 3.58 Åand 2.66 Åvs. 2.70 Å. The values slightly smaller than those of ref. [35], are likely due to the inclusion of long-range dispersion corrections in our calculations.

Before considering the structures Dimer H-bond adsorbed on Au(1 1 1), it is interesting to describe some properties of such dimer of methanethiol molecules in vacuum. In the latter case, we have found the optimum SH···SH and S-S distances: $d_{SH\cdots SH}$ = 2.53 Åand d_{S-S} = 3.65 Årespectively and the binding energy, $|E^{vacuum}_{dimerH-bond} - 2E_{Met}|$, equal to 0.13 eV. This binding energy is smaller (by a factor of 2) than for two water molecules (obtained at the same level of approximation and also in vacuum), as expected due to the less electronegative character of S compared with O. In addition, this value (0.13 eV) agrees well with the energy obtained for the most attractive minimum-energy configuration found for a dimer of $HSCH_3$ in vacuum through highly-accurate quantum chemistry calculations (i.e. 12.2 KJ/mol ∼0.126 eV) [36], which provides additional support to our method.

As mentioned above, in Dimer-H-bond structures one of the molecules is far from the energetically optimum configuration of a monomer. Thus, it is expected that the relatively small binding energy of the dimer H-bond in vacuum (0.13 eV) would entail a stability of the Dimer-H-bond structures much smaller than Monomers and Dimers. However, the results reported in Table 3 clearly show that this is not the case. At low coverages, the Dimer-H-bond structures ($\varepsilon\sim$ 0.70 eV) are in general, only slightly less stable than Monomers and Dimers ($\varepsilon\sim$ 0.74 eV). Moreover, due to the scarce coverage-dependence of ε for Dimers-H-bond structures, they become notably more stable than Monomers and Dimers for $\theta\gtrsim 1/6$.

The somewhat surprising coverage-independent adsorption energy per molecule of Dimer-H-bond structures (for $\theta\leq 1/3$) is due to the geometry of the Dimer-H-bond moiety. It involves two molecules quite close to each other, and one of them is further away from the surface than the other. Accordingly, the average surface area effectively occupied by a Dimer-H-bond moiety is significantly smaller than twice the surface area occupied by a Monomer. Thus, even for a coverage as large as $\theta = 1/3$, it is possible to accommodate on the surface (avoiding short range intermolecular repulsions) a larger number of molecules than in the case of Monomer and Dimer structures in which all the molecules are at the same height above the surface. Dipole-dipole interactions might also play some role on the coverage-dependence of the adsorption energy (see e.g. [37]) of each kind of structures we have considered, however, a detailed analysis of these effects is beyond the scope of the present paper.

Table 4
Idem Table 3 but for Chain-H-bond structures (see text).

θ	Unit cell	N	d_{S-S} (Å)	d_{S-Au} (Å)	$d_{SH\cdots SH}$ (Å)	ε (eV)
1/6	$2\times3\sqrt{3}$	2	3.59; 3.86	2.51; 4.62	2.25; 2.51	−0.62
	$2\times2\sqrt{7}$	2	3.60; 3.86	2.50; 4.60	2.25; 2.50	−0.63
1/3	$3\times3\sqrt{3}$		3.72; 3.86	2.58; 4.77	2.46; 2.57	−0.60
	$2\times2\sqrt{7}$		3.63; 3.81	2.53; 4.75	2.32; 2.44	−0.58

Dimer-H-bond structures certainly owe this somewhat surprisingly high stability to a cooperative effect between the molecules and the surface. For the molecule closest to the surface the S-surface bond becomes more stable due to the formation of the SH···SH H-bond, as indicated by d_{S-Au} values ∼0.08 − 0.30 Åsmaller than for Monomers and Dimers: $d_{S-Au}\sim 2.51-2.55$ Å vs. $d_{S-Au}\sim 2.59-2.85$ Å. This is certainly connected with the weakening of the S-H bond of the H-donor molecule due to the formation of the intermolecular H-bond which in turn, becomes stronger than in vacuum. In line with these arguments, both the S-S and the SH···SH distances in the Dimer H-bond structure are respectively 0.22 Åand 0.25 Åshorter than for a similar dimer in vacuum. Interestingly, the value of d_{S-S} we have obtained (i.e. d_{S-S}= 3.65 Å) is in excellent agreement with the one reported in ref. [14] for a Au_{20} cluster.

To quantify the role of this cooperative effect, we have taken the lowest energy configuration of the Dimer-H-bond structure found in the 2×4 unit cell, and we have computed the adsorption energy for each molecule individually (i.e. at the same position as in the Dimer-H-bond but removing the other molecule). The adsorption energy computed this way is −0.72 eV for the molecule closest to the surface, and −0.40 eV for the other. Thus, the sum of both adsorption energies is equal to −1.12 eV, i.e. 0.29 eV higher (less favorable) than the total adsorption energy of the Dimer-H-bond moiety for which we obtain −1.41 eV. If we subtract to 0.29 eV, the binding energy of the Dimer-H-bond in vacuum (i.e. 0.13 eV), we might attribute to purely cooperative *three-body* (molecule 1 - molecule 2 - surface) interactions, a stabilization of the Dimer-H-bond moiety of 0.16 eV. This is due to both intermolecular H-bond and (H-donor-molecule)-surface enhanced attractions.

In order to further illustrate the cooperative effect that provides stabilization to Dimer-H-bond structures, in Figure 3 we plotted the electronic density difference, $\Delta\rho$, for a Monomer (upper panels) and a Dimer-H-bond moiety (lower panels). Here, $\Delta\rho$ is the difference between the electronic density of the Monomer (Dimer-H-bond moiety) adsorbed on the surface, and the sum of the electronic densities of the surface and the Monomer (Dimer-H-bond moiety) in the same configurations but far from each other. In particular we have plotted iso-density surfaces corresponding to $|\Delta\rho|$ = 0.002, 0.005, and 0.01 e/Å^3 (negative and positive values of $\Delta\rho$ are represented in blue and green respectively). It is interesting to note that upon adsorption, there is a electronic charge redistribution around the S atom and its closest Au atom due to the formation of the S-surface bond. It is observed in particular, an increase of the electronic density along the S-Au axis and a consequent decrease of the electronic density between the most involved Au atom and its nearest neighbor Au atoms (see left panels), as well as between the S atom and the H atom bound to it (see left and middle panels). This is expected because the formation of the S-Au bond upon adsorption, necessarily entails some weakening of the other bonds in which participate both atoms. All these features are, in the case a Dimer-H-bond moiety, slightly more prominent than for the Monomer. For instance, the volume enclosed by the blue iso-surfaces of $\Delta\rho$ for the Dimer-H-bond moiety are slightly bigger than for the Monomer. Still, the differences between both cases are very small and can hardly be observed in a first sight of

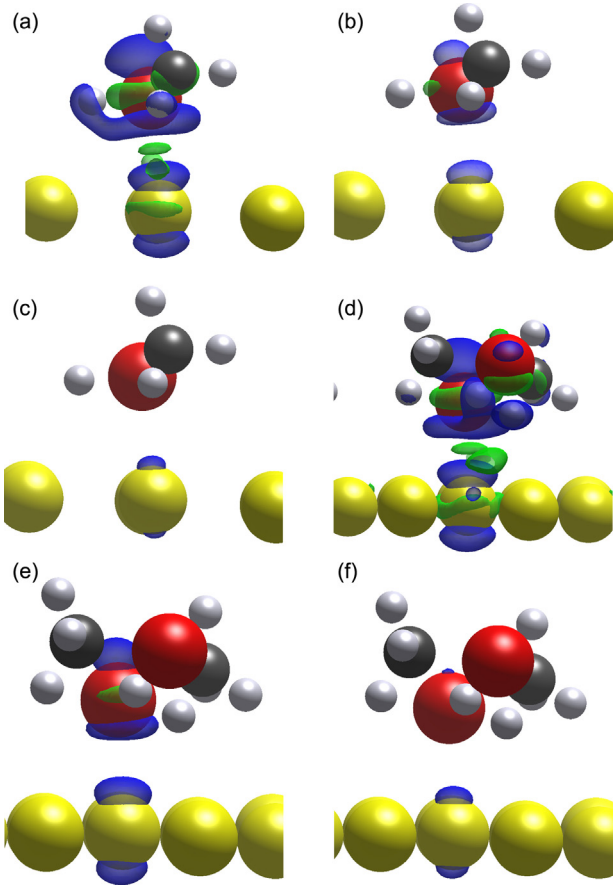

Fig. 3. Electronic density difference, $\Delta\rho$, for a Monomer: top panels, and a Dimer-H-bond moiety: bottom panels (see text). From left to right, the panels correspond to iso-density surfaces $|\Delta\rho|$ = 0.002, 0.005, and 0.010 e/Å^3. Negative and positive $\Delta\rho$ values are represented in blue and green respectively. S, C, H, and Au atoms are represented in red, grey, white, and yellow respectively. (For interpretation of the references to color in this figure legend, the reader is referred to the web version of this article.)

Figure 3, as expected because of the relatively weak character of the cooperative effect.

We have also investigated chains of molecules bond to each other through SH···SH H-bonds (Fig. 1d). In contrast with the Dimer-H-bond structures, in the chains the SH groups act simultaneously as H-donor and H-acceptor. This provokes a larger difference between the height above the surface of the two non-equivalent S atoms in the chain with respect to the Chain-H-bond structures (see e.g. Fig. 1d). The shortest S-Au distance for both Dimer-H-bond and Chain-H-bond structures are very close to each other: ~2.5 Å. In contrast, the S-surface distance for the molecule that is further away from the surface in the Chain-H-bond structures (~4.7 Å) is larger than in the case of Dimer-H-bond structures (3.8 Å). This certainly entails a weaker interaction of the molecules with the surface and the lower stability of the Chain-H-bond structures.

In order to determine the coverage range in which each kind of structure (or a mix of them) corresponds to the ground state of the system, it is convenient to plot the adsorption energy per molecule ε as a function of θ^{-1} [38] as shown in Figure 4. In particular, we have plotted the ground state curve for each *family* of structures (dashed lines) and the ground state curve of the system (full line). The ground state (GS) of the system corresponds to Monomer structures for $\theta \lesssim 1/8$ and a mix of Monomer and Dimer-H-bond structures for $1/8 \lesssim \theta \lesssim 1/3$ with a fraction of Dimer-H-bond moieties increasing with coverage [38]. For the lowest coverages considered, the small

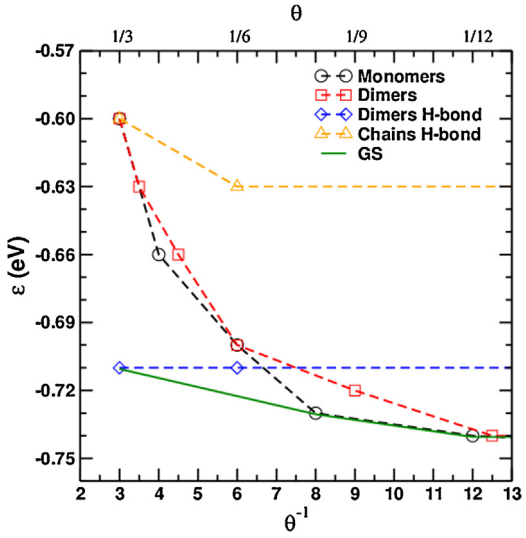

Fig. 4. Adsorption energies of the structures shown in Tables 1, 2, 3 and 4, as a function of $1/\theta$. The dashed lines corresponds to the ground state curve for each family structure and the full line to the ground state of the whole system.

energy difference between Monomer and Dimer structures, and entropic effects not accounted for when only the GS curve of the system is considered, do not rule out the observation of Dimers as reported in ref. [8]. However, our results clearly point to Dimers-H-bond as the most expected species to be observed for higher coverages (e.g. $\theta \sim 1/3$).

It might be argued that this conclusion could be a consequence of the approximations involved in the present calculations (e.g. DFT-D approach [25], PAW method [17]). In order to check this, all the structures were also studied at the same level of approximation as in ref. [34], i.e. without including dispersion forces and using ultrasoft pseudo potentials [39]. The adsorption energies per molecule obtained this way are smaller than the ones reported here by a factor ~2 because of the lack of long-range molecule-surface and (in a less extent) molecule-molecule van der Waals attraction. However, the conclusion that for $\theta \gtrsim 1/6$, Dimer-H-bond structures are more stable than Monomers, Dimers and Chain-H-bond ones remains unchanged. Moreover, without including long-range dispersion effects, the most stable Dimer-H-bond structure for coverages $\theta = 1/6$ and 1/3, are found for the unit cell $2\times2\sqrt{7}$ as seen in Table 3. Interestingly, the energy difference between Dimer-H-bond and Chain-H-bond structures are smaller when long range van der Waals forces are not included because the molecule-surface interaction for the molecule that is further away from the surface barely contributes to the stability of both structures involving H-bonds.

In Figure 5 we show the most stable Dimer-H-bond structure we have found for θ=1/3, with 4 molecules per $2\times2\sqrt{7}$ cell. We have labeled the sulfur atoms of the molecules with "a" and "d" to indicate those that play the role of H-acceptor and H-donor respectively. Though the energy difference between all the Dimer H-bond structures for θ=1/3 is very small, the lowest energy structure found (Fig. 5), is characterized by the symmetry observed in two independent experiments [9,10] for a full monolayer of molecularly adsorbed methanethiol molecules on Au(1 1 1) at low temperatures. It must be mentioned however, that the STM images obtained in the latter experiments were associated with a structure characterized by only 2 $HSCH_3$ molecules per $2\times2\sqrt{7}$ cell (i.e. $\theta = 1/6$, see e.g. Fig. 7 of ref. [9] and Fig. 2e of ref. [10]). Still, these observed STM images might be also compatible with our denser structure (θ=1/3) of the full monolayer (Fig. 5) if we assume that each dimer appears as a single protrusion in the images.

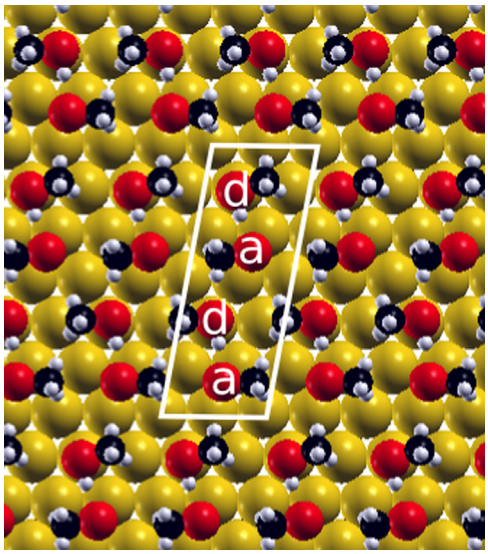

Fig. 5. Dimer-H-bond structure for θ = 1/3 with four molecules per 2 $\times 2\sqrt{7}$ unit cell. The type 'a' labels the H-acceptor molecules, and 'd', the H-donor ones. S, C, H, and Au atoms are represented in red, grey, white, and yellow respectively. (For interpretation of the references to color in this figure legend, the reader is referred to the web version of this article.)

In the light of the previous results, it is important to investigate in what extent a Dimer-H-bond state can act as a precursor for the S-H bond scission process. Whereas it is well established that molecularly adsorbed methanethiol molecules do not give rise to Au-adatoms [9,10], there is consensus on their prominent role in the stability of the full-coverage self-assembled monolayers of alkylthiolates on Au(1 1 1) (see e.g. [40]). However, it is unknown in what extent Au-adatoms can play a role during the S-H bond scission process itself. So, a study of the activation energy for the S-H bond scission without considering the role of Au ad-atoms is still reasonable and useful [34]. Then, we have computed the minimum energy dissociation pathway for S-H bond cleavage on a ideal Au(1 1 1) surface starting from a Dimer H-bond state through which the H-donor molecule transfers the H atom of the thiol group to the H-acceptor molecule that simultaneously transfers its H atom to the surface (i.e. H-transfer mechanism). The minimum energy pathway obtained is schematically represented in Figure 6a. For comparison, in Figure 6b we have also included the minimum energy pathway for the S-H dissociation through a unimolecular mechanism [34], computed at the same level of approximation. The activation energies obtained (with respect to the molecularly adsorbed state) for the H-transfer and the unimolecular mechanism are 0.78 eV and 0.88 eV respectively. Thus, the Dimer-H-bond is not only the most stable molecularly adsorbed state for $\theta \gtrsim 1/6$ but also (slightly) facilitates the S-H bond scission through a concerted H-transfer channel. Concerning the role of long range dispersion corrections, as mentioned above, they strongly stabilize molecularly adsorbed states. However, they barely modify the energy of both transition states with respect to the molecular state. It might

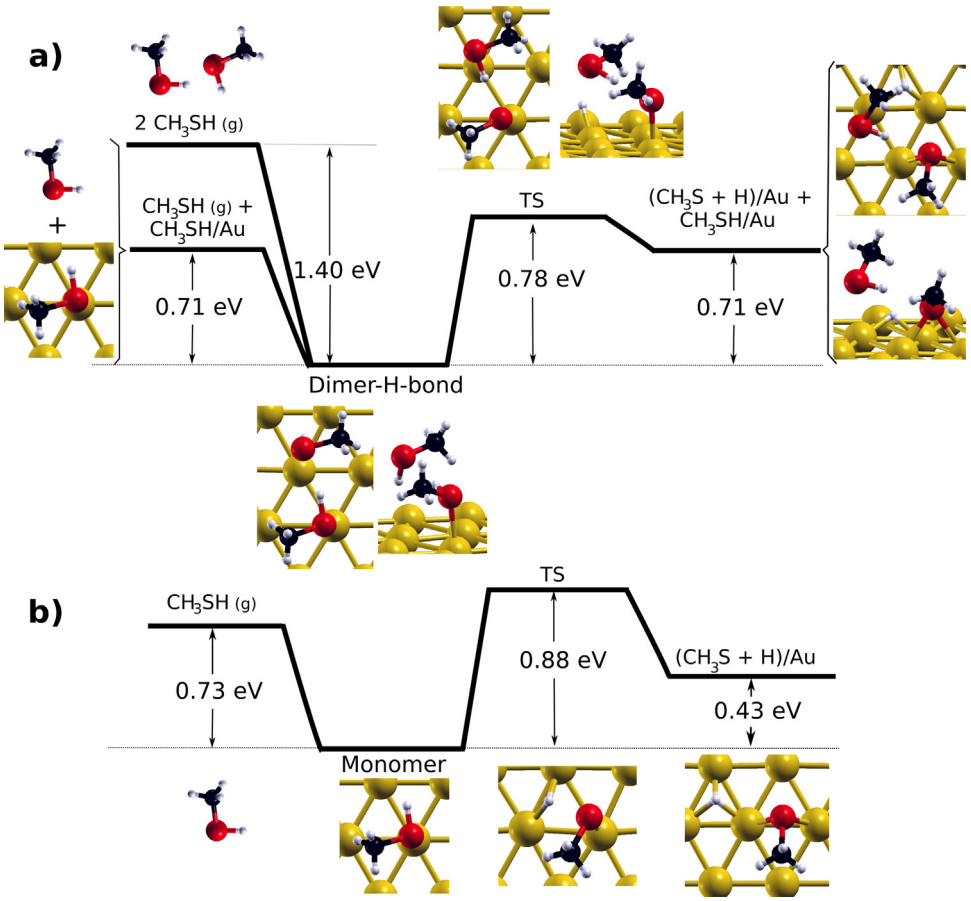

Fig. 6. Energetics along the dissociation pathways for the S-H bond cleavage through a cooperative H-transfer mechanism (a), and through an unimolecular mechanism (b). S, C, H, and Au atoms are represented in red, grey, white, and yellow respectively. (For interpretation of the references to color in this figure legend, the reader is referred to the web version of this article.)

be argued that the obtained 0.1 eV difference in activation energies (i.e. 0.78 eV vs. 0.88 eV) is similar to the typical errors of DFT calculations. However, it must be also noted that for $\theta\sim$ 1/3, molecularly adsorbed methanethiol molecules must form Dimer-H-bond moieties instead of being adsorbed as Monomers. Thus, our results allow us to predict that at large coverages (e.g. $\theta\sim$ 1/3), the H-S bond cleavage process is dominated by a H-transfer mechanism.

4. Conclusions

In this paper, we have investigated and compared the stability of a large set of structures of methanethiol molecularly adsorbed on Au(1 1 1) through Density Functional Theory calculations with and without long-range dispersion corrections. We have carried out a systematic study in a large range of surface coverages and focused on possible cooperative effects between molecules through intermolecular H-bond interactions. In particular, we have investigated four kind of structures: Monomers, Dimers, Dimers-H-bond, and Chains-H-bond. We conclude that the ground state of the system corresponds to Monomer structures for $\theta \lesssim 1/8$ and for higher coverages, a mix of Monomers and Dimer-H-bond moieties. In particular, near the saturation coverage (i.e. for one monolayer of methanethiol characterized by the coverage θ=1/3) Dimer-H-bond structures are significantly more stable than all the others considered. We show that this is a direct consequence of a SH$\cdots$SH H-bond interaction which on the surface, becomes significantly stronger than in vacuum due to a reinforcement of the S-Au bond for one of the molecules forming the Dimers. Moreover, we have also found that Dimers-H-bond can act as a precursor for the S-H bond cleavage process through a concerted H-transfer mechanism which is characterized by an activation energy barrier $\sim$0.1 eV smaller than the one found for a unimolecular pathways. Thus, cooperative effects between methanethiol molecules would start playing a prominent role at the very early stages of the grow of self-assembled monolayers (SAMs) of alkanethiols on Au(1 1 1). We expect that these results will stimulate new experimental investigations intended to elucidate the actual role of H-bond interactions for the formation of SAMs of short chain alkanethiols on Au(1 1 1).

References

[1] A. Ulman, Chem. Rev. 96 (1996) 1533.
[2] F. Schreiber, Prog. Surf. Sci. 65 (2000) 151.
[3] J. Love, L.A. Estroff, J. Kriebel, R. Nuzzo, G. Whitesides, Chem. Rev. 105 (2005) 1103.
[4] C. Vericat, M. Vela, R. Salvarezza, Phys. Chem. Chem. Phys. 7 (2005) 3258.
[5] P. Maksymovych, O. Voznyy, D.B. Dougherty, D.C. Sorescu, J.T. Yates Jr., Progr. Surf. Sci. 85 (2010) 206.
[6] C. Vericat, M. Vela, G. Benitez, P. Carro, R. Salvarezza, Chem. Soc. Rev. 39 (2010) 1805.
[7] L. Ferrighi, Y.-x. Pan, H. Grönbeck, B. Hammer, J. Phys. Chem. C 116 (2012) 7374.
[8] P. Maksymovych, D. Sorescu, D. Dougherty, J. Yates Jr., J. Phys. Chem. B. 109 (2005) 15992.
[9] P. Maksymovych, D.B. Dougherty, Surf. Sci. 602 (2008) 2017.
[10] G. Nenchev, B. Diaconescu, F. Hagelberg, K. Pohl, Phys. Rev. B 80 (2008) 081401(R).
[11] L.D. Colebrook, D.S. Tarbell, Chemistry 47 (1961) 993.
[12] S.H. Marcus, S.I. Miller, J. Am. Chem. Soc. 88 (1966) 3719.
[13] S.M. Russell, D.-J. Liu, M. Kawai, Y. Kim, P.A. Thiel, J. Chem. Phys. 133 (2010) 124705.
[14] M. Askerka, D. Puchugina, N. Kuz'menko, A. Shestakov, J. Phys. Chem. A 116 (2012) 7686.
[15] M.C. Payne, M.P. Teter, D.C. Allen, J.D. Joannopoulos, Rev. Mod. Phys. 64 (1992) 1045.
[16] J.P. Perdew, K. Burke, M. Ernzerhof, Phys. Rev. Lett. 77 (1996) 3865.
[17] P.E. Blöchl, Phys. Rev. B: Condens. Matter 50 (1994) 17953.
[18] M. Methfessel, A.T. Paxton, Phys. Rev. B 40 (1989) 3616.
[19] H. Monkhorst, D. Pack, Phys. Rev. B 13 (1976) 5186.
[20] G. Kresse, J. Hafner, Phys. Rev. B 47 (1993) 558.
[21] G. Kresse, J. Hafner, Phys. Rev. B 49 (1994) 14251.
[22] G. Kresse, J. Furthmüller, Comput. Mater. Sci. 6 (1996) 15.
[23] G. Kresse, J. Furthmüller, Phys. Rev. 54 (1999) 11169.
[24] G. Kresse, D. Joubert, Phys. Rev. B 59 (1999) 1758.
[25] S. Grimme, J. Comput. Chem. 27 (2006) 1787.
[26] K. Tonigold, A. Gross, J. Chem. Phys. 132 (22) (2010) 224701.
[27] D. Lide, CRC Handbook of Chemistry and Physics, 81st edn., CRC Press, Boca Raton, FL, 2001.
[28] C. Kittel, Introduction to Solid State Physics, John Wiley & Sons, New York, 1971.
[29] G. Mills, H. Jónsson, Phys. Rev. Lett. 72 (1994) 1124.
[30] G. Mills, H. Jónsson, G. Schenter, Surf. Sci. 324 (1995) 305.
[31] H. Jónsson, G. Mills, K.W. Jacobsen, in: B.J. Berne, G. Ciccotti, D.F. Coker (Eds.), Classical and Quantum Dynamics in Condensed Phase Simulations, World Scientific, Singapore, 1998.
[32] D. Sheppard, R. Terrell, G. Henkelman, J. Chem. Phys. 128 (2008) 134106.
[33] G. Henkelman, H. Jónsson, J. Chem. Phys. 113 (2000) 9978.
[34] P. Lustemberg, M. Martiarena, A. Martínez, H. Busnengo, Langmuir 24 (2008) 3274.
[35] J.-G. Zhou, Q.L. Williams, F. Hagelberg, Phys. Rev. B 76 (2007) 075408.
[36] S. Garrison, S. Sandler, J. Chem. Phys. 123 (2005) 054506.
[37] A. Kokalj, Phys. Rev. B 84 (2011) 045418.
[38] P.N. Abufager, G. Zampieri, K. Reuter, M.L. Martiarena, H.F. Busnengo, J. Phys. Chem. C 118 (2014) 290.
[39] D. Vanderbilt, Phys. Rev. B 41 (1990) 7892.
[40] P.N. Abufager, J.G. Solano Canchaya, Y. Wang, M. Alcamí, F. Martín, L. Alvarez Soria, M.L. Martiarena, K. Reuter, H.F. Busnengo, Phys. Chem. Chem. Phys. 13 (2011) 9353.